We are IntechOpen, the world's leading publisher of Open Access books Built by scientists, for scientists

4,800
Open access books available

122,000
International authors and editors

135M
Downloads

Our authors are among the

154
Countries delivered to

TOP 1%
most cited scientists

12.2%
Contributors from top 500 universities

WEB OF SCIENCE™

Selection of our books indexed in the Book Citation Index in Web of Science™ Core Collection (BKCI)

Interested in publishing with us?
Contact book.department@intechopen.com

Numbers displayed above are based on latest data collected.
For more information visit www.intechopen.com

Chapter 4

Electromagnetic Waves Propagation and Detection in Shielded Dielectric Power Cables

Chunchuan Charles Xu and Chengyin Liu

Additional information is available at the end of the chapter

http://dx.doi.org/10.5772/61055

Abstract

Partial discharge occurs a lot in shielded dielectric power cables. Partial discharge pulses are high-frequency electromagnetic waves that propagate in the shielded dielectric power cables. This chapter will study partial discharge propagation and detection in shielded dielectric power cables.

Keywords: Propagation, Detection, Shielded Power Cables

1. Introduction

1.1. Shielded dielectric power cables

Since the 1970s, shielded dielectric cables have been used overseas, and since the mid-1980s, they have been extensively used in North America as well. Today, because of environmental concerns, shielded solid dielectric cables are used more and more and most new power cables installed are solid dielectric cables. Figure 1 [1] shows the structure of a typical high-voltage shielded dielectric power cable. The conductor core F is the part that delivers power. The conductor shields C and E help smooth the electric field between the conductor and the insulation materials. The dielectric or insulation D is used to insulate high-voltage core F from the ground, i.e. neutral wires B. Encapsulating jacket A prevents water and dust from getting into the cable.

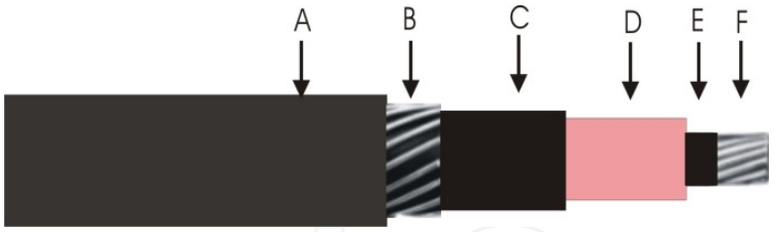

Figure 1. A typical high-voltage extruded solid dielectric cable. A, encapsulating jacket; B, neutral wires; C, ground shield; D, dielectric; E, conductor shield; F, conductor; the conductor shield and ground shield are semiconductive. Usually, they are made by adding carbon black into a polymer and the particle size of the carbon black ranges from 15 to 50 nm. The basic function of this configuration is to confine the electric field within the cable and obtain a symmetrical radial distribution of the electric within the dielectric [1].

1.2. Partial discharge in shielded dielectric power cables

Most failures occurring in the shielded dielectric cables are related to partial discharge. Partial discharges are localized breakdowns in a small portion of the insulations, which can be solid or fluid electrical insulation. When high voltage is applied to high-voltage equipment, defects introduced during the manufacturing process such as contained insulation cracks, contained insulation surfaces, or voids can all lead to partial discharges. In some cases, even without any defects, aging can cause the degradation of the insulator leading to partial discharges. PD makes damage to the equipment, and equipment with PD occurring within will eventually fail after a certain time depending on the strength of the PD if proper treatments are not applied. It's important to monitor partial discharges in high-voltage systems and if PD is detected, appropriate actions should be taken to prevent sudden failures, which can cause big blackouts.

Figure 2 gives us some basic ideas on how partial discharges occur. The cavity in the insulation normal contains gas which could be ionized when the electrical field exceeds the cutoff strength. When this happens, electromagnetic waves in the radiofrequencies are generated along with light, heat, noise, and possibly gas. With appropriate technologies and by detecting the HF radio signals, the magnitude as well as the location of partial discharges can be identified and used for assessing the health status of the shielded dielectric cable.

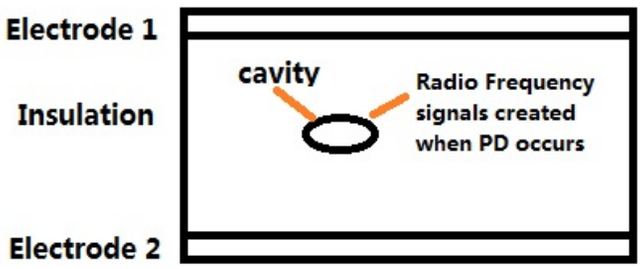

Figure 2. A "typical" partial discharge mechanism. The cavity in the insulation normally contains gas, which could be ionized when the electrical field exceeds the cutoff strength.

http://dx.doi.org/10.5772/61055

2. Electromagnetic wave propagation in shielded dielectric cables

2.1. Partial discharge pulse properties

As discussed above, PD can create high-frequency electromagnetic waves in the radiofrequencies, heat, light, gas, etc. A lot of research has been conducted to study for detecting PD using sensors for heat, light, gas, etc. In this chapter, we focus on radiofrequency high-frequency PD signal detection as it provides a way to detect PD over long distances, which makes it useful in many cases. To effectively detect and analyze PD, first we have to understand the PD pulse. The authors will analyze the PD pulse spectrums, frequency properties, etc. Note that PD occurring in different high-voltage apparatus varies significantly due to the insulation properties and electric stress needed for triggering PD. Since this chapter focuses on PD in shielded dielectric cables, we will focus on the PD pulse properties in shielded dielectric cables.

Because the formation of electron avalanches is within the nanosecond range, the PD event is associated with a very fast current pulse. As of today, there is no direct way to measure the PD current pulse. A lot of theories have been proposed to simulate and study the current pulse and different measuring techniques were developed to measure PD current pulses. The PD is caused by the flow of the electrons and ions. The moving speed of the electrons is much faster than the ions. Some early theoretical simulations [2–5] predicted that the pulse current in the voids of the shielded dielectric cables has a rising time and pulse widths in the nanosecond range followed by a long-duration, low-magnitude pulse. Figure 3 shows one theoretically predicted PD current pulse. With the high-speed oscilloscope available, some PD experiments were conducted by Fujimoto and Boggs (1981) and Boggs and Stone (1982) [4] and the experimental results agree with the theoretical simulation results.

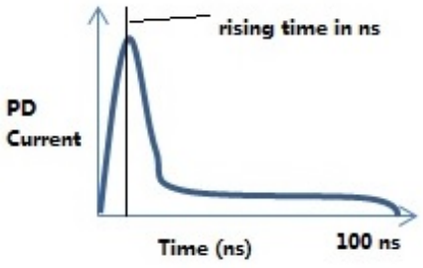

Figure 3. One theoretically predicted PD current pulse [2–5].

There is no standard spectrum chart for PD pulses in the power cables because under different situations, the PD pulse can be in different shapes leading to different energy spectrums. Some experimental results [6] show that the partial discharge spectrum has a peak point at about 100 MHz when measuring PD at a distance very close to the PD source. When the partial discharge pulse propagates in the high-voltage cable, its high-frequency components are attenuated by the losses majorly caused by the semiconducting materials and, after a 100-meter trip, the peak frequency of the spectrum can be reduced to 20–30 MHz.

2.2. Shielded dielectric cable HF attenuation properties

When the electromagnetic PD wave propagates in the cable, its HF components are significantly attenuated by the shielded cables. How far the pulse can travel and be detected by the PD detection devices heavily relies on the attenuation properties of the cable. A lot of research [7–17] has been conducted to study different aspects of the HF attenuation features of the shielded dielectric cables. From Figure 1, the HF attenuation is caused by various components. One measurement result [9] shown in Figure 4 gives HF attenuation losses for different components for different frequencies. From Figure 4, it can be seen that for this measurement, conductor and neutral wire skin effect losses dominate for low frequencies up to 5 MHz. After 5 MHz, grounding shielding losses as well as the dielectric losses start to play a more important role. This can be explained by the fact that at low frequencies, the capacitive current is low thus the current passing through the dielectric, conductor and ground shielding is low leading to relatively low losses. When frequencies are higher, the larger capacitive current flowing through the resistive component of the conductor and ground shielding makes big losses.

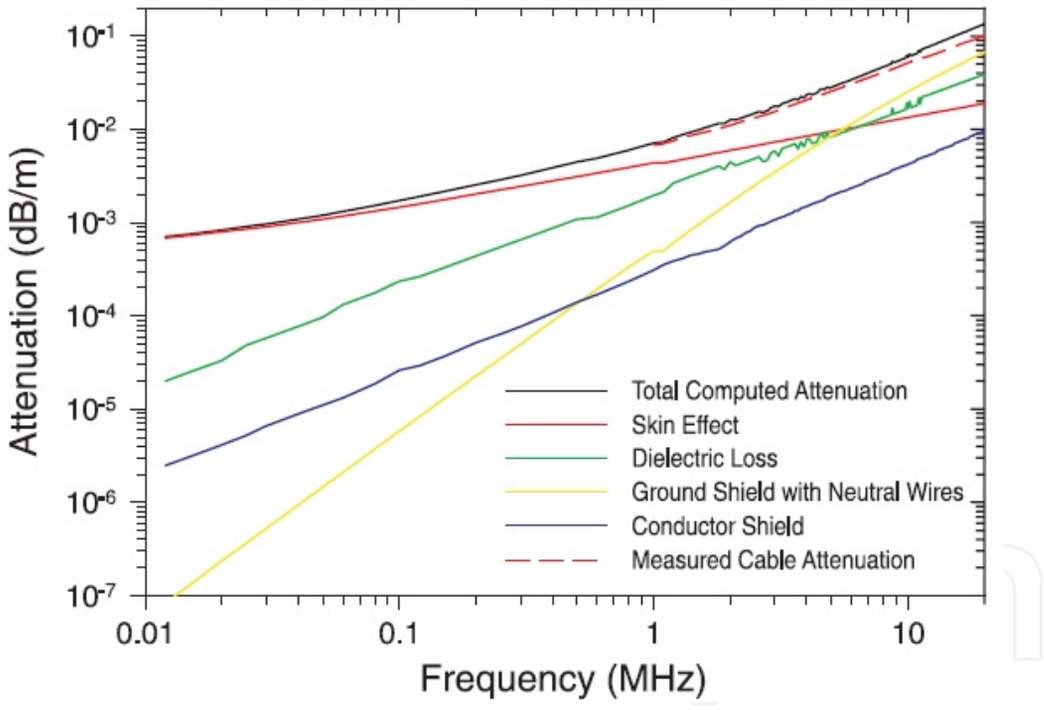

Figure 4. Measurement results for one shielded cable [9].

2.2.1. Shield HF property measurements

From the above analysis, it can be seen that the dielectric properties of the shielding are critical to HF losses of the shielding dielectric cables. The dielectric properties of the cable semiconducting shielding can be measured by a HF impedance analyzer. Figure 5 [10 and 17] shows a typical measurement configuration for HF dielectric properties (dielectric constant and

http://dx.doi.org/10.5772/61055

conductivity) of the cable shielding. Conducting electrodes with small surface resistivity, often metal paint, are applied to the two surfaces of the shield material. Normally, contact with the electrodes is made along one edge of the sample. There is a voltage drop across the "conducting" electrodes, which can cause errors in the dielectric properties measurement when the current flowing through the sample and the nonperfect electrode resulting in possible measurement errors.

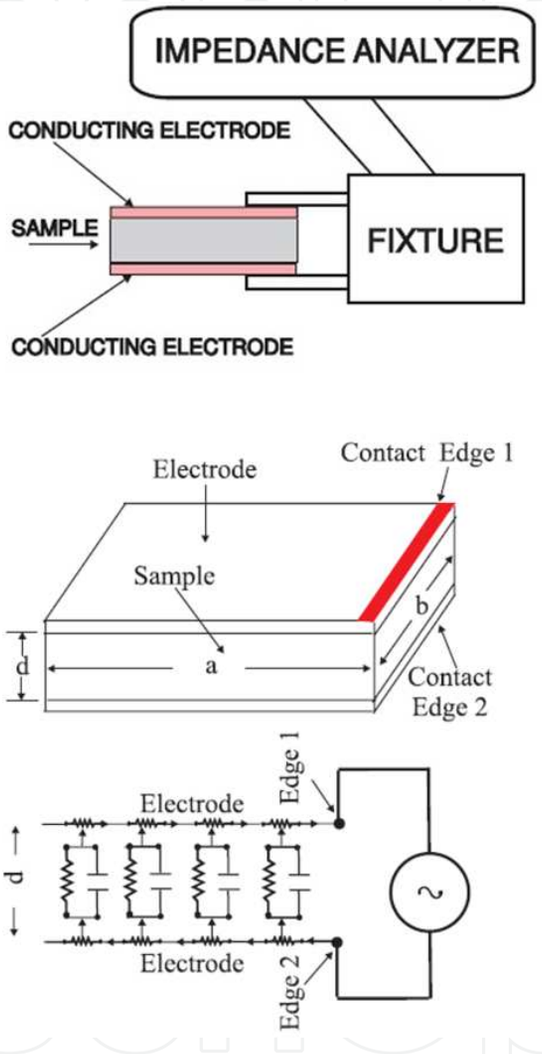

Figure 5. Typical measurement method for HF dielectric properties of the cable shielding and a simplified sample geometry and lumped element representation [10 and 17].

The measured sample impedance is normally interpreted as resulting from the dielectric constant and conductivity of the sample if we assume that the losses and voltage drop in the electrodes are negligible [7 and 10]. The applied electrode has a finite conductivity (normal silver paint) resulting in changes in the measured loss leading to errors in predicting the shield properties. These errors increase with frequency because the current through the electrodes increase significantly with frequency as a result of the large dielectric constant of the shield material. If we assume that voltage is applied along one edge of the upper and lower surface

of a rectangular sample, as shown in Figure 5, and define $I1(x)$ is the current as a function of distance from that edge on one surface (electrode), then the magnitude of the current in the other surface is also $I1(x)$ with an opposite direction. Likewise, if the voltage on energized surface as a function of distance from that edge is $U1(x)$, then the voltage on the grounded surface is Uo-$U1(x)$. Uo is the applied voltage. From the geometry shown in Figure 5, the following equations can be derived

$$l_1(x) = -\frac{U_0\sqrt{\frac{Ab}{2\rho}}\left\langle \exp\left(x\sqrt{\frac{2\rho A}{b}}\right) - \exp\left[(2a-x)\sqrt{\frac{2\rho A}{b}}\right]\right\rangle}{\left[1+\exp\left(2a\sqrt{\frac{2\rho A}{b}}\right)\right]}$$

$$U_1(x) = \frac{U_0}{2}\left\langle \frac{\exp\left(x\sqrt{\frac{2\rho A}{b}}\right) + \exp\left[(2a-x)\sqrt{\frac{2\rho A}{b}}\right] + \exp\left(2a\sqrt{\frac{2\rho A}{b}}\right)+1}{1+\exp\left(2a\sqrt{\frac{2\rho A}{b}}\right)}\right\rangle \tag{1}$$

$$A = \frac{b(\sigma + j\omega\varepsilon\varepsilon_0)}{d}$$

where d is the sample thickness, ρ is the electrode surface resistivity in Ω/sq, a is the sample length, b is the sample width, ω is the angular frequency, and σ and ε are the conductivity and dielectric constant of the sample, respectively. Furthermore, we can derive the measured conductivity and relative dielectric constant as [17]

$$\sigma_P = \frac{(2P_{electrode} + P_{shield})d^2}{VU_0^2} \tag{2}$$

and

$$\varepsilon_P = \frac{dI_c}{U_0\omega\varepsilon_0 ab} \tag{3}$$

From Eq. 2, it can be seen that the power losses $P_{\text{electrode}}$ caused by the electrodes cause errors as we are measuring losses by the shield P_{shield}, not losses by the electrodes. On the other hand, there is a voltage drop along the electrode due to the larger current and finite conductivity of the electrode resulting in some areas where there is no current flowing through. Thus, the measured losses can be larger or smaller than the actual shield losses. The shield conductivity property measurements affect cable high-frequency attenuation calculations a lot, thus it's very important that we minimize the errors caused by the electrode resistance. A first-order estimate of the maximum frequency to which accurate measurements are likely by using the DC conductivity and low frequency shield dielectric constant to roughly estimate the maximum

http://dx.doi.org/10.5772/61055

frequency at which the impedance of the shield is comparable to that of the sample electrodes resulting in Equation 4 for a rectangle sample and Equation 5 for a circular sample [10 and 17]:

$$f_{\max} = \frac{\sqrt{-4\sigma^2\rho^2a^2 + \left(\frac{d}{a}\right)^2}}{4\pi a\rho\varepsilon\varepsilon_0} \tag{4}$$

$$f_{\max 1} = \frac{\sqrt{-\sigma^2\rho^2 \ln\left(\frac{r_2}{r_1}\right)^2 + \left(\frac{d}{r_2^2 - r_1^2}\right)^2}}{2\pi \ln\left(\frac{r_2}{r_1}\right)\rho\varepsilon\varepsilon_0} \tag{5}$$

where r_2 is the "conducting" electrode radius, r_1 is the contact radius at the center of the electrode, and d is the sample thickness. Figure 6 shows the measured ground shield relative dielectric constant and conductivity for a shield power cable as well as the calculated and measured HF attenuation for the shielded cables.

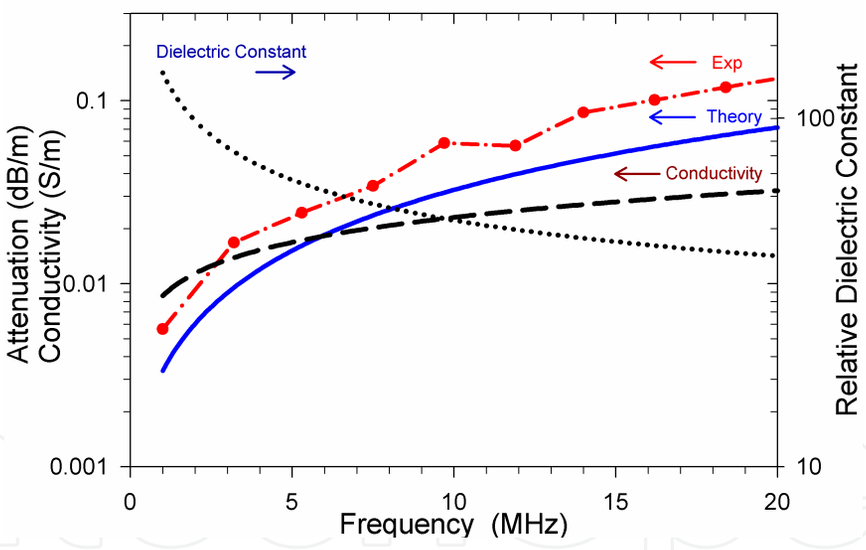

Figure 6. The measured ground shield relative dielectric constant and conductivity for a shielded power cable.

2.2.2. Shielded cable HF attenuation calculations

From Figure 4, there are losses from different components of the shielded power cable. The losses come from insulation, skin effect, conduct shield, and ground shield. For high frequencies (5–20 MHz), the loss in the ground shield could dominate the shield cable loss [11,12]. This chapter discusses the loss calculations in the ground shield as it dominates losses at high frequency, which is critical for HF PD pulse propagation, detection and analysis. The shielded

power cable can have different geometries, configurations, and number of neutral wires. The chapter won't cover all cable configurations. Two typical shielded cables will be studied.

2.2.2.1. Normal jacketed shield power cable HF loss calculations

The conductor and ground shield layers of shielded distribution cables help provide a smooth interface between conductors and insulation. Since the losses caused by the conductor shield are pretty small compared to the losses in other components, these losses are sometimes ignored in analyses. Figure 7 shows a typical jacketed shielded cable geometry and its simplified computation model [11 and 17]. The current flows from the conductor through the insulation (dielectric) passing through the ground semiconducting shield before it reaches the neutral, resulting in big losses in the shield at high frequency. The current passing through the ground shield is determined by the conductor voltage level and dielectric impedance, and can be considered as a "current source."

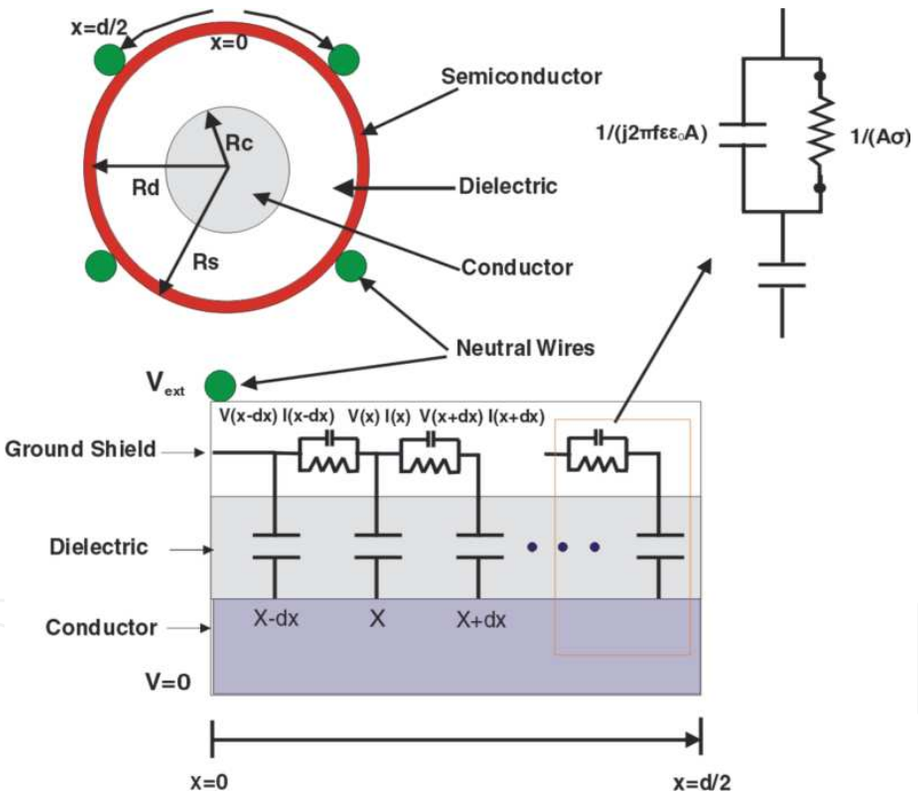

Figure 7. A typical jacketed shielded cable geometry and its simplified computation model [11 and 17]. The current flows from the conductor through the insulation (dielectric) passing the ground semiconducting shield before it reaches the neutral resulting in big losses in the shield at high frequency.

The loss caused by the current in the ground shield, including the component caused by the propagation of the current in a circumferential direction to reach a neutral wire, can be calculated with known cable parameters.

http://dx.doi.org/10.5772/61055

With this simplified model, the ground shield current and voltage distributions of such a system can be derived [11 and 17]:

$$V(x) = -\frac{V_0\left\{\exp\left(x\sqrt{\frac{K_1}{K_2}}\right)+\exp\left[(d-x)\sqrt{\frac{K_1}{K_2}}\right]\right\}}{\left[1+\exp(d\sqrt{\frac{K_1}{K_2}})\sqrt{K_2}\right]}$$
$$I(x) = \frac{V_0\left\{\exp\left[(d-x)\sqrt{\frac{K_1}{K_2}}\right]-\exp(x\sqrt{\frac{K_1}{K_2}})\right\}}{\left[1+\exp(d\sqrt{\frac{K_1}{K_2}})\right]\sqrt{K_1K_2}} \quad (6)$$
$$K_1 = \frac{1}{(\sigma_3 + j\omega\varepsilon_0\varepsilon_3)T}$$
$$K_2 = \frac{T_2}{\sigma_4 + j\omega\varepsilon_0\varepsilon_4} - \frac{2j\pi R_s}{\omega C}$$

where d is the circumferential distance between two neutral wires; V_0 is the applied external voltage; x is the position along the circumference of the ground shield; σ_3 is the conductivity of the ground shield; ε_3 is the dielectric constant of the ground shield; σ_4 is the conductivity of the conductor shield; ε_4 is the dielectric constant of the conductor shield; ω is the angular frequency of the applied voltage; C is the capacitance of the insulation per meter; R_s is the radius of the ground shield; T is the thickness of the ground shield; and T_2 is the thickness of the conductor shield. From Figure 7, it is the current that passes through the resistive component of the grounding shield that causes losses. To find the loss, the current through the resistive component needs to be derived, which is given by [11 and 17]

$$I_{r1} = \frac{j\sigma_3 I(x)}{j\sigma_3 - \omega\varepsilon_0\varepsilon_3} \quad (7)$$

and similarly, the current passing through the resistive component of the conductor shield can be found as

$$I_{r2} = \frac{j\sigma_4 I_c(x)}{j\sigma_4 - \omega\varepsilon_0\varepsilon_4} \quad (8)$$

With these two currents known, the losses in the conductor and ground shields can be found by calculating the power dissipation, i.e. the product of I_{r1} and I_{r2} and the resistance of the ground and conductor shields. With some math software such as Maple program and integrating the product of current and the resistive components, the amount of power dissipated can be found. To make it easy for the reader to perform such calculations, the Maple program is attached in the Appendix.

The losses in the ground shield with some typical parameters (neutral wire conductor radius of 4 mm, dielectric thickness of 7 mm, conductor shield thickness of 0.2 mm, and ground shield thickness of 0.5 mm, the relative dielectric constant of 200, and conductivity of 0.1 S/m) can be seen in Figure 8 for a different number of neutral wires. Finite analysis element calculations are also conducted and the results of which are compared with the analytic results. They agree with each other well.

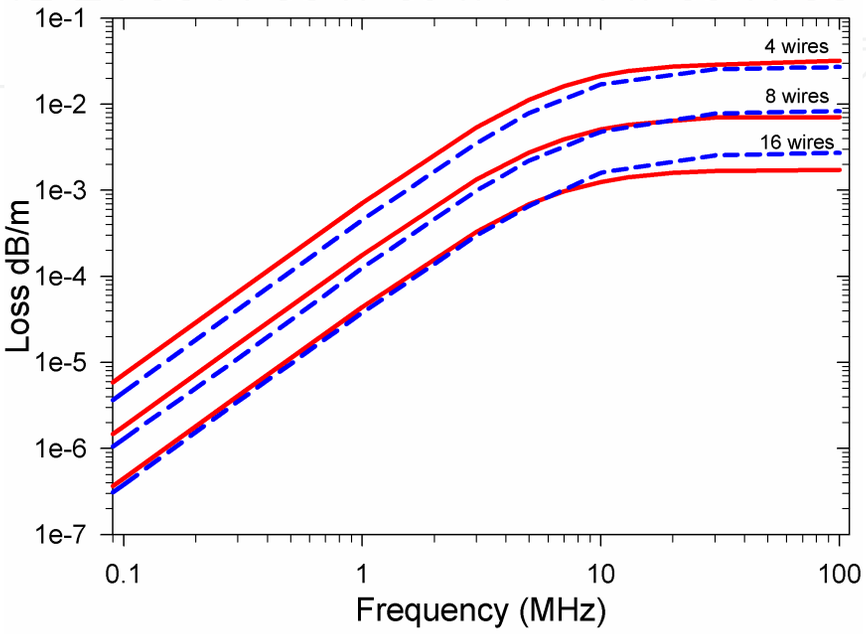

Figure 8. Losses in the ground shield for different numbers of neutral wires [11 and 17]. Finite analysis element calculations are also conducted and the results of which are compared with the analytic results. They agree with each other well.

To give the reader a better idea on the total HF losses in the shielded power cable, one more plot is given in Figure 9 for a cable with six neutral wires [11 and 17]. From Figure 9, it can be seen that for high frequencies (from 5 to 20 MHz), the ground shield loss, including the losses caused by the interaction of the ground shield with the neutral wires, dominates the HF loss for this six neutral-wire cable. The interaction of the neutral wires with the ground shield plays a critical role for the total loss, as can be seen by comparison with the line showing the ground shield loss with and without the effect of the circumferential current.

2.2.2.2. Unjacketed shield power cable HF loss calculations

To save costs, sometimes, unjacketed cables are installed. A cable jacket ensures intimate contact between ground shield and neutral wires. For unjacketed cables, this contact is not ensured resulting in the loss caused by the ground shield as a function of the separation between the neutral wires and the ground shield and the distance between points of contact of the neutral wires with the ground shield [13]. This section will address the loss as a function of neutral wire separation from the ground shield, contact interval between the neutral wires,

http://dx.doi.org/10.5772/61055

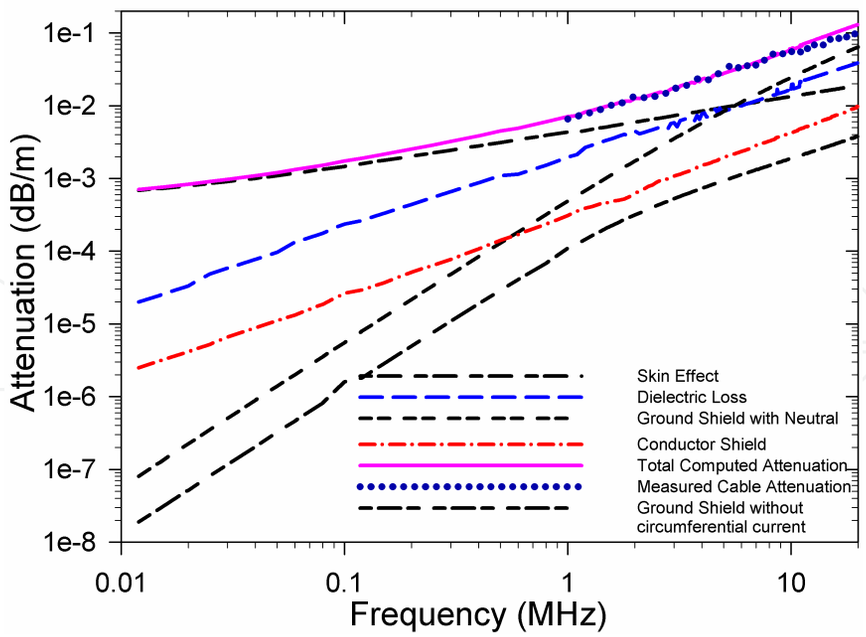

Figure 9. The total losses in a cable with six neutral wires. The losses from the current flowing through the ground losses contribute significantly to the total loss.

ground shield dielectric properties, frequency, etc. Figure 10 [13] gives a simplified model for the unjacketed cable.

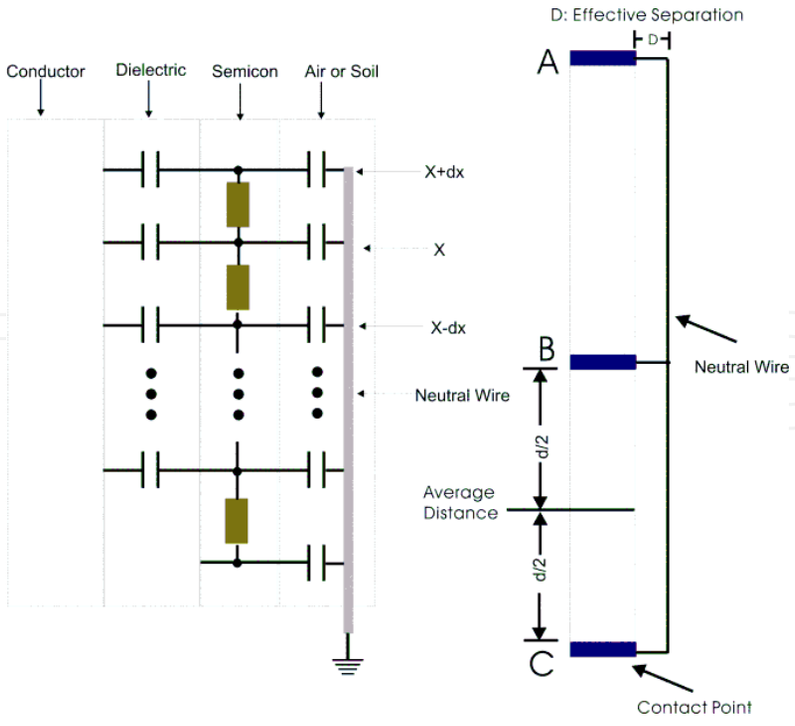

Figure 10. A simplified model for the unjacketed cable. Due to the nature of unjacketed cables, the neutral wires only have contacts with certain points, A, B and C.

Due to the nature of unjacketed cables, the neutral wires only have contacts with certain points, A, B, and C. Similar to a normal jacketed cable, the current flowing through resistive component of the ground shield leads to loss that dominates the loss for high frequencies. The voltage and current distributions as well as the current passing through the resistive component of such a system can be found as [13]

$$
\begin{aligned}
V(x) &= -\frac{V_0\left(Z_c + Z_c\exp(-d\sqrt{K1}) + Z_{c1}\left\{\exp\left(-x\sqrt{K1}\right) + \exp\left[(x-d)\sqrt{K1}\right]\right\}\right)}{(Z_{c1}+Z_c)\left[1+\exp\left(-d\sqrt{K1}\right)\right]},\\
I(x) &= \frac{V_0\sqrt{Z_{c1}(Z_c+Z_{c1})}\left\{\exp\left(-x\sqrt{K1}\right) - \exp\left[(x-d)\sqrt{K1}\right]\right\}}{\left[(Z_{c1}+Z_c)\left(1+\exp\left(-d\sqrt{K1}\right)\right)\right]\sqrt{Z_sZ_c}},\\
K1 &= \frac{Z_s(Z_{c1}+Z_c)}{Z_{c1}Z_c}\\
Z_c &= \frac{-j\ln\left(\frac{R_d}{R_c}\right)}{2\omega\pi\varepsilon\varepsilon_0}\\
Z_{c1} &= \frac{-j}{\omega C_{tl}}\\
Z_s &= \frac{\sigma - j\omega\varepsilon_1\varepsilon_0}{8\pi R_d T\left[\sigma^2 + (\omega\varepsilon_1\varepsilon_0)^2\right]}
\end{aligned}
\tag{9}
$$

$$
I_{r1} = \frac{(\sigma^2 - j\sigma\omega\varepsilon_0\varepsilon_1)I(x)}{\sigma^2 + (\omega\varepsilon_0\varepsilon_1)^2} \tag{10}
$$

Similarly to a normal jacketed cable, the losses can be found by integrating the product of the resistive current and the resistance. The Maple program is similar to the normal jacketed shield cable and can be found in paper [13], and thus is not given in this chapter. The ground shield losses in the unjacketed cable, which dominates the HF loss, can vary a lot for different shield dielectric constants, conductivity, and thickness of the ground shield. The thickness of the ground shield plays an important role because the displacement current from the conductor to the ground shield flows longitudinally through the resistance of the ground shield before it reaches a neutral wire-ground shield contact. This loss is maximized under the condition that the resistive impedance of this path is comparable to the capacitive impedance of the dielectric, which is significantly affected by the thickness of the ground shield. For a typical ground shield thickness of 1 mm, and conductor radius, 3.62 mm; insulation thickness, 4.83 mm; capacitance between ground shield and neutral wires, 150 pF/m; insulation dielectric constant, 2.2; distance between two neutral wire-ground shield contacts, 3 cm; frequency, 20 MHz, the loss of such a jacketed cable vs. dielectric constant and conductivity is shown in

Figure 11 [13]. From Figure 11, it can be seen that the losses can be pretty large due to the long distance needed for the displacement current to flow before it reaches the neutral wires, which means that the HF electromagnetic PD wave can be attenuated significantly in the unjacketed cable.

As stated at the beginning of this section, shield cables have different geometries and configurations. The authors won't address too many configurations and only two typical shielded cables, i.e. jacketed normal shielded cable and unjacketed shielded cables, are studied in this section. The reader should keep in mind that when designing and analyzing the HF electromagnetic PD wave signals, it's very important to know the shield dielectric properties and cable actual geometry and configurations to get a rough idea of the cable's HF attenuation properties. The readers should also know that it's not easy to do the HF dielectric property measurements and use caution when conducting such measurements. Furthermore, the reader needs to know that the shields in the cables are under pressure whereas the shields under test have no pressure. Some compensation might be necessary to offset the pressure difference.

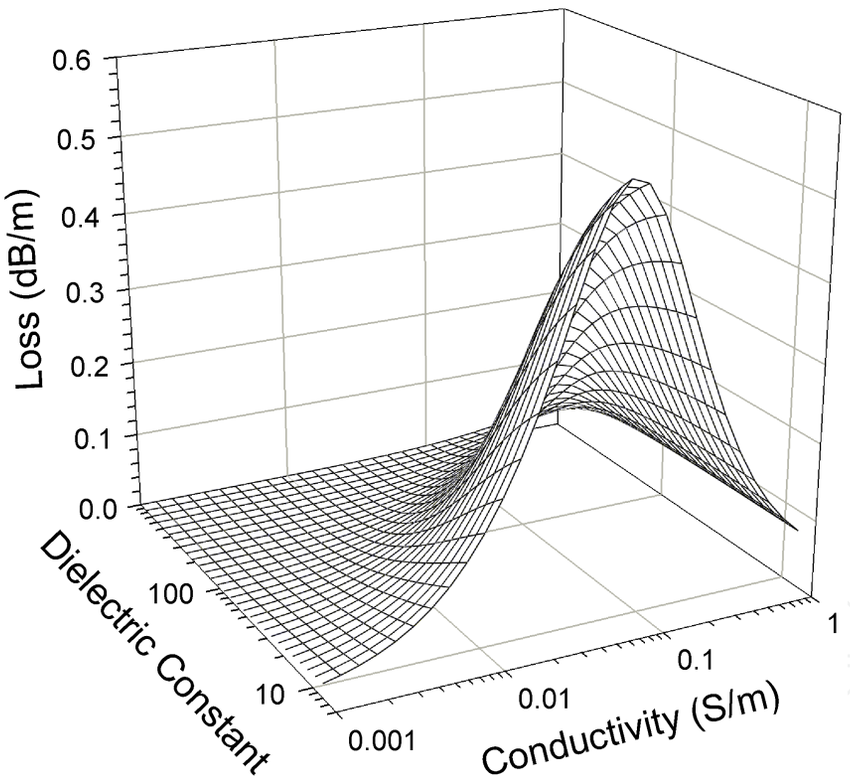

Figure 11. Losses vs. dielectric constant and conductivity for typical parameters.

2.3. HF electromagnetic PD wave propagation

The HF electromagnetic PD wave propagates in the shield cable and the wave is attenuated while it travels. How significant the wave is is mainly determined by the HF loss properties of the cable, which has been discussed extensively in Section 2.2. Besides the losses of the cable,

the cable splices and termination can also affect the wave propagation and attenuation. Figure 12 shows one typical PD wave propagation. The PD wave propagates in both directions passing through the cable splices before it reaches the cable termination and reflects back if the waves are not attenuated completely. When it travels along the cable, HF components are most attenuated due to the facts discussed in Section 2.2, because the displacement current increased with frequency resulting in higher losses for higher frequencies. This provides the electromagnetic wave pulse a big pulse width as shown in Figure 12. If the pulse is not attenuated completely, it will reach the cable termination and reflect backward toward the PD source as shown in Figure 12. To analyze the effect of the cable losses, the electromagnetic wave pulse can be treated as a Gaussian pulse. If a Gaussian pulse in time domain is applied at the left end of the cable to simulate the PD source signal, it will propagate through the splices before it can reach the termination. For simplicity, splices are thought in parallel with loads having characteristic impedance. Since we apply a Gaussian pulse in time domain, we need to transform it to the frequency domain, multiply it with attenuation factor caused by splices in frequency domain, then transform it back to time domain. The output voltage is attenuated by a factor of Vatt which is

$$Vatt = \frac{2Z}{Z + Z_c}, Z = \frac{Z_s Z_c}{Z_s + Z_c} \tag{11}$$

where Z_s is splice effective impedance, Z_c is characteristic impedance. By doing so, we get loss vs. number of splices as shown in Figure 13. Parameters used in computation are given in the caption of Figure 13. We also can treat the problem by calculating the energy dissipated by the cable. Current flows through semicon will result in loss. By calculating the loss, we can get a voltage attenuation ratio in frequency domain, Vatt1, which is:

$$Vatt1 = \sqrt{1 - \frac{P_L}{P_I}} \tag{12}$$

where P_L is the power dissipated by splice whereas P_I is the input power. A Gaussian pulse multiplied by this ratio results in an attenuated Gaussian pulse as seen in Figure 14.

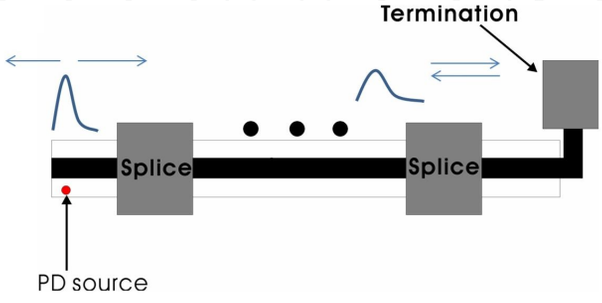

Figure 12. One typical PD wave propagation pattern. Note that the wave propagates in both directions although only the right section is shown here.

http://dx.doi.org/10.5772/61055

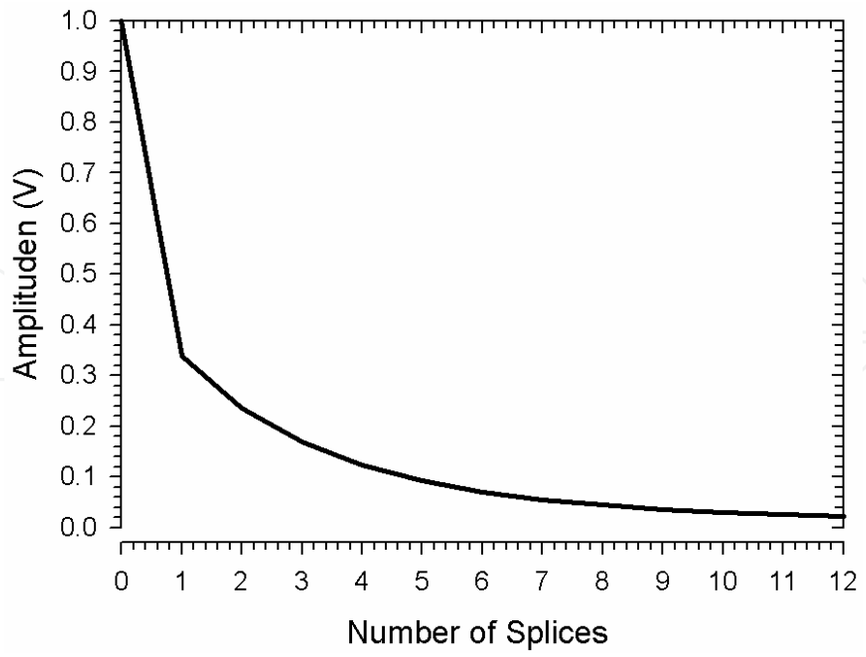

Figure 13. Amplitude as a function of number of splice number. Splices have the following parameters: length, 60 cm; semicon conductivity, 5 s/m; conductor radius, 4 mm; thickness of the insulation, 4 mm; thickness of semicon, 6 mm; dielectric constant of semicon, 300; dielectric constant of insulation, 2.2.

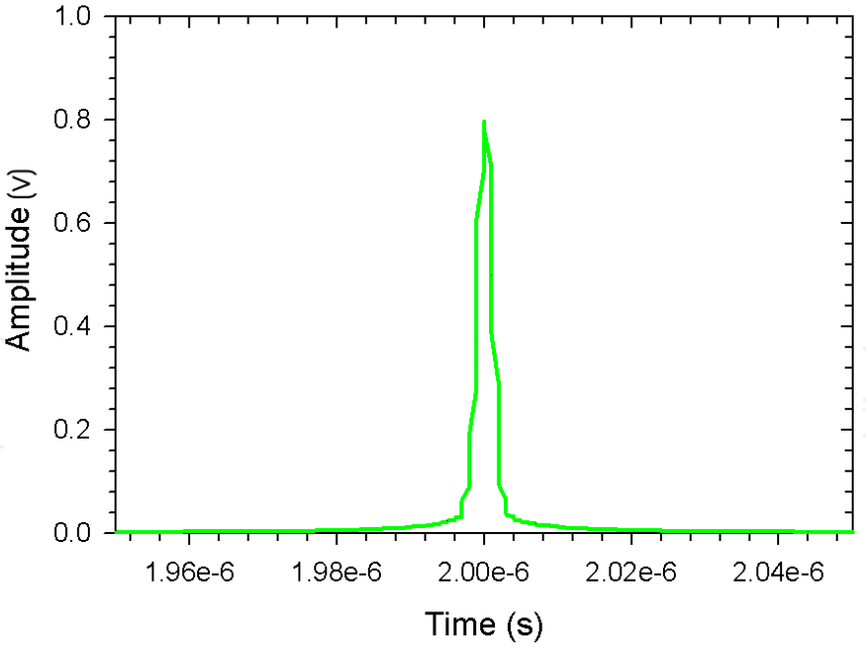

Figure 14. Attenuated Gaussian pulse. The splice has the following parameters: radius of conductor, 1 cm; thickness of insulation, 0.5 cm; thickness of semicon, 0.3 cm; conductivity of semicon, 10 S/m; dielectric constant of semicon, 300; dielectric constant of insulation, 3.3; distance of splice, 40 cm.

The reader should keep in mind that the studied case is a simulation result based on some assumed shield dielectric properties. To assess the losses caused by the splices, some field measurements as well as further computations are necessary. Normally, the splices have smaller losses compared with the long cable.

3. Electromagnetic wave detection in shielded dielectric cables

PD detection has been extensively used for high-voltage apparatus diagnostic and status assessment. This section focuses on electromagnetic PD wave detection as, due to its relatively smaller losses, the HF PD signal can propagate for a long distance and can be detected by the PD sensors located either at the termination or other appropriate locations of the power circuit for the shielded power cables.

3.1. PD pulse sensor

Different sensors (optical, acoustic, electrical, etc.) are used for detecting the PD. For detecting the electromagnetic waves propagating in shielded dielectric cables, normally a high-frequency current transformer (HFCT) and ultra high-frequency (UHF) sensor are used [18–21]. The HFCT is normally placed around the shielded cable or sometimes around the ground strip to collect the PD signals. The UHF sensor captures the UFH electromagnetic waves propagating in the shielded cable, which can be attenuated quickly depending on the loss characteristic of the cable. Figure 15 shows some typical configurations for using HFCT in the PD measurements. There are a lot of different other sensors such as coupling capacitor, inductively coupled probes, integrated partial discharge sensor, etc. that are used in PD electromagnetic pulse detections. Among them, the HFCTs are one of the most widely used sensors due to their high bandwidth and ease of use.

For processing the measured PD signals, different theories and algorithms have been proposed for optimizing PD testing results [18–21]. For partial discharge measurements, as stated in the above sections, the PD signals cannot be detected directly due to its nature as the PD is inside the insulation. The electromagnetic wave pulse signals we capture are indirect measurements of the PD and analysis needs to be done to extract useful information such as PD locations, PD magnitude, etc. Some PD detection technologies require an excitation voltage to produce a partial discharge signal pulse to find the PD location. For locating the PD location, two sensors are placed at two different locations along the cable and if the attenuation along the cable is the same, then when the two sensors reads the same level of PD, the PD source is in the middle of the two sensors assuming that the cable splices contribute little or few losses for the PD pulse propagation. Theoretically, the technology should work but an excitation voltage could damage the cable and the cable needs to be taken out of service. More and more PD detection systems have been developed for online real-time measurements as they don't require dangerous excitation voltages and can be used to assess the HV apparatus under more realistic conditions. However, the highly noisy environment caused by the high voltage and high current of the power cable makes extracting useful PD information difficult. To improve the

http://dx.doi.org/10.5772/61055

signal-to-noise ratio for optimized measurement results, different technologies, such as noise filtering, digital signal processing optimization, signal amplifying, etc., are used.

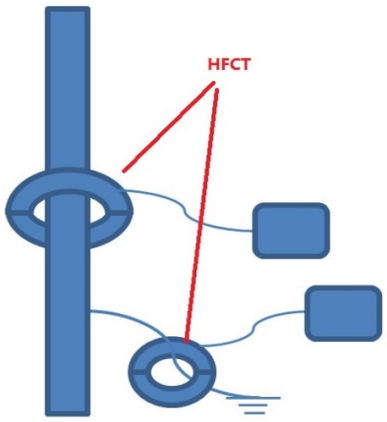

Figure 15. HFCT used in PD detection.

3.2. PD pulse detection data processing and transmitting

Some PD detection systems detect PD at the hot spots identified by the utility companies and can't be used to monitor the system continuously due to the complicated data processing and communication. Due to the fact that the PD signals are normally HF signals which can attenuate quickly if a normal coaxial cable is used for connecting the PD detection sensor and the PD signal analyzer and also for safety concerns, sometimes, optical coupling [22] is used for long-distance data transmitting between the sensor and the PD data analyzer. After the field signals are received by data processors, which can be a wide-band oscilloscope or a spectrum analyzer, the PD data are processed for waveform, phase, span, etc. [28]. For better results, field signals can also be filtered and amplified and processed with specialized processing computers for trend analysis and alarm generation, etc.

With the advancement of modern wireless communication and digital signal processing technologies, real-time continuously online PD detection becomes more realistic [23-28]. Different wireless technologies have been used for transmitting measured processed data back to the controlling center. The processed output from the oscilloscope or other digital instruments can be fed into data transmitters using Ethernet, wireless LTE modem, Wifi, Zigbee network, etc. Ethernet is reliable and easy to use but sometimes it can be unavailable. Wireless LTE is flexible but can be expensive due to its common monthly data fee. Wifi is also a good option if it's available. Zigbee is a low-cost and low-maintenance method compared with cellular data service as it does not have a monthly fee. The Zigbee node is small and, if set correctly, it can run for a long time without maintenance. Figure 16 shows one customized Zigbee node [29]. However, its data rate is relatively low compared with Ethernet and Wifi. To monitor the PD in real time, the captured PD signals can be processed with a wideband local oscilloscope or other devices such as a spectrum analyzer and the output can be fed into

one of the data transmitting routers. The PD measurements will lead to a lot of raw data and normally they can't be sent directly to the remote controlling center due to its high data volume. After processing, the data can be sent back to the controlling and data concentrator for appropriate actions such as cable maintenance, alarm generation, etc.

Figure 16. One Zigbee node.

4. Summary and discussion

Because the shielded power cables are widely used in modern HV power systems and the fact that the partial discharge is a powerful tool for assessing the HV power system status, HF PD electromagnetic wave propagation, detection, and analysis have been extensively studied. In this chapter, the authors look into the details of the shield power cable structure, their HF attenuation properties, PD electromagnetic wave propagation, and address the detection and analysis of the HF electromagnetic wave in the shielded power cable.

Appendix: Maple program for loss calculations in a typical jacketed shielded cable

```
>restart;

>Rc:=4e-3:# Rc is the conductor radius.

>epsilon:=2.2:#Epsilon is the dielectric constant of the insulation.

>epsilon0:=8.85e-12:

>mu1:=1*4*Pi*1e-7:

>Rs:=11.7e-3: #Rs is the ground shield radius (m).

>Rd:=11.2E-3:#Rd is the insulation radius (m).
```

http://dx.doi.org/10.5772/61055

>V0:=1:

>N:=4:# N is the number of neutral wires.

>omega:=2*Pi*f:

>epsilon0:=8.85e-12:

>l:=1:# let the length of the cable be 1 m;

>T:=0.5e-3:# T is the thickness of the ground shield.

>T2:=0.2-3:# T2 is the thickness of the conductor shield.

>d:=evalf(2*Pi*Rs/N):# d is the length between two neutral wires.

>C:=2*Pi*epsilon*epsilon0*l/(ln(Rs/Rc)):# Capacitance of the insulation per meter.

>C1:=2*Pi*epsilon*epsilon0/(ln(Rd/Rc)):

>L1:=mu1*ln(Rs/Rc)/(2*Pi):

>Zc:=evalf(sqrt(L1/C1)):#Characteristic impedance.

>K1:=1/((sigma3+omega*epsilon0*epsilon3*I)*l*T):

>K2:=-2*I/omega/C/1*Pi*Rs+T2/(sigma4+omega*epsilon4*epsilon0*I)/1:

>I1:=

-V0*(exp(1/K2^(1/2)*K1^(1/2)*x)-exp(-K1^(1/2)*(-d+x)/K2^(1/2)))/K1^(1/

2)/K2^(1/2)/(1+exp(1/K2^(1/2)*K1^(1/2)*d)):#

Current distribution along the ground shield.

>V1:=-V0*(exp(1/K2^(1/2)*K1^(1/2)*x)+exp(-K1^(1/2)*(-d+x)/K2^(1/2)))/K2^(

1/2)/(1+exp(1/K2^(1/2)*K1^(1/2)*d)):#

90

Voltage distribution along the ground shield.

>I2:=(-V1)/K2:# Current flowing through the conductor shield.

>dZr4:=T2/(sigma4*l*dx):# dZr4 is the elemental resistive impedance of the conductor shield.

>dZc4:=1/(I*omega*(epsilon0*epsilon4*l*dx/T2)):# dZc4 is the elemental capacitive impedance of the conductor shield.

>Ratio2:=simplify(dZc4/(dZc4+dZr4)):# To get the current flowing through the resistive component of the conductor shield, we calculate Ratio2.

>Irtotal2:=I2*Ratio2:# Irtotal2 is the current flowing through resistive component

of the conductor shield.

>dZr3:=(1*dx)/(sigma3*l*T):# Same as above.

>dZc3:=1/(I*omega*(epsilon0*epsilon3*l*T/dx)):# Same as above.

>Ratio1:=simplify(dZc3/(dZc3+dZr3)):# Same as above.

>Irtotal:=I1*Ratio1:# Irtotal1 is the current flowing through resistive component of the ground shield.

>Ii:=Im(Irtotal):

>Ir:=Re(Irtotal):

>Ii2:=Im(Irtotal2):

>Ir2:=Re(Irtotal2):

>Pd4:=int(((Ir2)^2+(Ii2)^2)*(T2/(sigma4)),x=0..d/2):# Conductor shield power dissipation

>Pd3:=int(((Ir)^2+(Ii)^2)*(1/(sigma3*T)),x=0..d/2):# Ground shield power dissipation

>Pin:=(V0)^2/Zc:# Input power.

>dB3:=10*log10(1-(Pd3*2*N/Pin)):# Ground shield attenuation.

>dB4:=10*log10(1-(Pd4*2*N/Pin)):# Conductor shield attenuation.

Author details

Chunchuan Charles Xu[1*] and Chengyin Liu[2]

*Address all correspondence to: xuchunchuan@gmail.com

1 Underground Systems, Inc, Armonk, NY, U.S.A.

2 Harbin Institute of Technology Shenzhen Graduate School, Shenzhen, China

References

[1] Chunchuan Xu, "Recent Developments in Power System Diagnostics and Protection: Partial Discharge Detection and Analysis." Recent Patents on Electrical & Electronic Engineering (Formerly Recent Patents on Electrical Engineering), Volume 3, Number 1, January 2010, pp. 51–54(4).

[2] Wolfgang Hauschild, et al. "High-Voltage Test and Measuring Techniques", Springer Heidelberg New York Dordrecht London. 2014.

[3] P. Degn, "Partial Discharges in Solid Dielectrics", Ph.D. Thesis, Electric Power Engineering Department, Technical Uni of Denmark, Lyngby, 1971.

[4] S. Boggs, et al. "Fundamental limitations in the measurement of corona and partial discharge", IEEE Transactions on Electrical Insulation, Volume EI-17, Issue 2, pp. 143–150, 1982.

[5] C.A. Bailey, "A study of internal discharge in cable insulation", IEEE Paper No. 31, pp. 66–363, 1966.

[6] Z. Liu, et al. "The Propagation of Partial Discharge Pulses in a High Voltage Cable", Proc. of AUPEC/EECON eds, 1999. Citeseer.

[7] G.C. Stone, et al. "Propagation of partial discharge pulses in shielded power cable," in 1982 Annu. Rep. Conf. Elect. Insul. Dielect. Phenomena. Washington, DC: Natl. Acad. Sci., pp. 275–280.

[8] W. L. Weeks, et al. "Wave propagation characteristics in underground power cable," IEEE Trans. PAS-103, (Oct) pp. 2816–2825, 1984.

[9] Chunchuan Xu, et al. "High Frequency Properties of Shielded Power Cable Part 1: Overview of Mechanisms", IEEE Electrical Insulation Magazine, Volume 21, Issue 6, pp. 24–28, 2005.

[10] Chunchuan Xu, et al. "High Frequency Properties of Shielded Power Cable Part 2: Sources of Error in Measuring Shield Dielectric Properties", IEEE Electrical Insulation Magazine, Volume 22, Issue 1, pp. 7–13, 2006.

[11] Chunchuan Xu, et al. "High Frequency Properties of Shielded Power Cable. Part 3: Loss from Neutral Wire–Shield Interaction", IEEE Electrical Insulation Magazine 04/2007; 23(2):12–16.

[12] Chunchuan Xu, et al. "High Frequency Loss from Neutral Wire–Shield Interaction of Shielded Power Cable", Power Delivery, IEEE Transactions on, Volume 23, Issue 2, 2008, pp. 531–536.

[13] Chunchuan Xu, et al. "High-Frequency Loss in Unjacketed Distribution Cable and Its Effect on PD Measurement", Power Delivery, IEEE Transactions on, Volume 24, Issue 2, 2009, pp. 495–500.

[14] Jim Jun Guo, et al. "High Frequency Attenuation in Transmission Class Solid Dielectric Cable", Power Delivery, IEEE Transactions on, Volume 23, Issue 4, 2008, pp. 1713–1719.

[15] M. Vakilian, et al. "Investigation of PD Signal Propagation Characteristics in XLPE Cables", International Conf. Power Syste. Techn., pp. 1863–1868, 2004.

[16] G. Mugala, et al. "High frequency characteristics of a shielded medium voltage XLPE cable," in 2001 Annu. Rep. IEEE Conf. Elect. Insul. Dielect. Phenomena, 2001, pp. 132–136.

[17] Chunchuan Xu, "High Field Phenomena in Polymer Films and High Frequency Attenuation in Shielded Power Cable", Ph.D thesis, Uconn 2007.

[18] M. Wild et al. "Power Cable Modeling for PD Pulse Propagation and Sensitivity", 2013 IEEE Electrical Insulation Conference (EIC), June 2–5, pp. 57–60.

[19] Khushboo Arora, et al. "Wavelet Analysis Used for Partial Discharge Pattern Recognition", International Journal of Emerging Technology and Advanced Engineering. Website: www.ijetae.com (ISSN 2250-2459 (Online), Volume 4, Special Issue 1, February 2014) pp. 125–130.

[20] Naima Oussalah, et al. "Analytic Solutions for Pulse Propagation in Shielded Power Cable for Symmetric and Asymmetric PD Pulses", IEEE Transactions on Dielectrics and Electrical Insulation Vol. 14, No. 5, October 2007, pp. 1264–1270.

[21] Xiaoli Zhou, et al. "The Application of Partial Discharge Detection for the condition assessment of XLPE Power Cables" Przegląd Elektrotechniczny (Electrical Review), ISSN 0033-2097, R. 88 NR 6/2012, pp. 313–316.

[22] Y. Tian, et al. "Continuous on-line monitoring of partial discharges in high voltage cables", Conference Record of the 2004 IEEE International Symposium on Electrical Insulation, 2004. 19–22 Sept. 2004 pp. 454–457.

[23] Marco Tozzi, "Partial Discharges in Power Distribution Electrical Systems: Pulse Propagation Models and Detection Optimization", PhD thesis, Alma Mater Studiorum–University of Bologna, 2010.

[24] Ghadir Madi, et al. "Impacts of impulsive noise from partial discharges on wireless systems performance: application to MIMO precoders", Madi et al. EURASIP Journal on Wireless Communications and Networking 2011, 2011:186.

[25] Shan, Qingshan, et al. "Performance of Zigbee in Electricity Supply Substations", International Conference on Wireless Communications, Networking and Mobile Computing, 2007. WiCom 2007. 21–25 Sept. 2007, pp. 3871–3874.

[26] S.A. Bhatti, et al "Vulnerability of Zigbee to Impulsive Noise in Electricity Substations", General Assembly and Scientific Symposium, 2011 XXXth URSI, 13–20 Aug. 2011, pp. 1–4.

[27] P.C. Baker, et al. "Data Management of On-Line Partial Discharge Monitoring Using Wireless Sensor Nodes Integrated with a Multi-Agent System", International Conference on Intelligent Systems Applications to Power Systems, 2007. ISAP 2007. pp. 1–6.

[28] Chen Rui-Long, et al. "The Design of Partial Discharge On-Line Monitoring System for XLPE Power Cable", Research Journal of Applied Sciences, Engineering and Technology 6(21): 4063–4069, 2013.

[29] Chengyin Liu, et al. "Development and validation of wireless strain sensor network", Conference Record of the 13th International Symposium on Structural Engineering, 2014, Oct. 24–27, Hefei, China.

IntechOpen

IntechOpen